Astron. Astrophys. 352, 517–531 (1999)

ASTRONOMY AND ASTROPHYSICS

High veiling at near infrared wavelengths in classical T Tauri stars

D.F.M. Folha[1,2] **and J.P. Emerson**[2]

[1] Centro de Astrofísica da Universidade do Porto, Rua das Estrelas, s/n – 4150 Porto, Portugal (dfmf@astro.up.pt)
[2] Department of Physics, Queen Mary and Westfield College, Mile End Road, London E1 4NS, UK (j.p.emerson@qmw.ac.uk)

Received 10 May 1999 / Accepted 2 November 1999

Abstract. The near infrared veiling (the ratio of any non-photospheric excess flux to the photospheric flux) is studied for a sample of 50 mainly Classical T Tauri stars (CTTS), mostly from the Taurus-Auriga complex, based on high resolution spectra ($\mathrm{R} \sim 20,500$) of wavelength regions in the J and K wavebands (near Paβ $-$ $1.28215\,\mu$m – and near Brγ $-$ $2.16611\,\mu$m respectively). The method used to compute the veiling at these wavelengths is independent of any assumptions about reddening/extinction towards the studied objects.

Photospheric absorption lines are identified in the spectra of 73% of the CTTS observed at J and in 71% at K. For these stars the veiling in the J (r_{J}) and K (r_{K}) wavebands was determined. Average values for all the stars are $\langle r_{\mathrm{J}} \rangle = 0.57$ and $\langle r_{\mathrm{K}} \rangle = 1.29$. Considering only stars with veilings determined to better than 3σ these means are $\langle r_{\mathrm{J}} \rangle = 0.97$ and $\langle r_{\mathrm{K}} \rangle = 1.76$. For the remaining 27% of the stars observed at J and 29% at K, for which no photospheric lines were identified, lower limits were obtained for r_{J} and r_{K}. Considering only those stars with lower limits the mean lower limits are $\langle r_{\mathrm{J}} \rangle > 1.34$ and $\langle r_{\mathrm{K}} \rangle > 2.4$. Our results indicate high veiling of these stars in the NIR. The NIR veilings deduced are considerably greater than expected from extrapolation of the veilings measured in the optical, assuming that they result from an accretion shock, and are also bigger than the expected veiling from an accretion disk. Although the origin of this large NIR veiling is not clear one possibility deserving further study is that it partially arises within shocks at the base of magnetospheric accretion columns which cover a large fraction of the stellar surface. The possibility that the near infrared veiling of photospheric lines is not caused by a continuum, but is rather due to non-photospheric line emission from the disk or from a shock at the base of the accretion columns, should also be investigated by detailed modelling including the Ti, Fe, Si & Mn lines as opacity sources.

Key words: stars: circumstellar matter – stars: formation – stars: pre-main sequence – infrared: general – infrared: stars

1. Introduction

Classical T Tauri stars (CTTS) are low mass pre-main sequence stars whose spectra may potentially include components arising in: a stellar photosphere, a shock where accreting matter falls onto the star, infalling material, an accretion disk, and possibly starspots and a residual circumstellar envelope. All these are then affected by interstellar extinction. One must disentangle the effects of these various components to understand the physical mechanisms by which matter accretes onto such a star. One useful method of avoiding the problems of poorly known extinction, which can dominate photometric attempts to separate the components, is to determine the strengths of photospheric lines relative to the continuum (from the photosphere together with all other sources). These strengths may be compared with those found in appropriate (non accreting) stars of the same spectral type which are (presumed to be) unaffected by accretion or disks and envelopes. Thus one can determine the ratio of the non-photospheric emission sources to the photospheric emission. This ratio is known as the veiling, and its determination allows confrontation with model predictions to improve our understanding of the mechanisms in accreting T Tauri (and other young) stars.

The veiling at a given wavelength (r_λ) is defined as the ratio of the excess flux to the stellar photospheric flux. It has been studied mainly in the optical region (e.g. Basri & Bertout 1989; Basri & Batalha 1990; Hartigan et al. 1991; Guenther & Hessman 1993; Valenti et al. 1993; Hartigan et al. 1995; Gullbring et al. 1998). The excess flux at optical wavelengths is thought to result from shocks where matter accretes onto the stellar surface. Models where these shocks arise at the base of magnetospheric accretion columns imply the shock veiling in the near-IR (NIR) should be less than 0.1 for typical (M0) CTTS parameters. (e.g. Calvet & Gullbring 1998).

Emission from the disks of T Tauri stars (TTS) is also not expected to produce significant veiling in the near infrared (NIR), as the inner holes that are thought to exist do not contain enough material to produce significant veiling (Meyer et al. 1997). Neither are the accretion rates through these disks likely to be high enough to produce the temperatures necessary to produce significant NIR veiling further out in the disks. Any veiling from the disk will be from gas, as dust will have sublimated at the temperatures where strong NIR fluxes would be radiated.

CO absorption features have been used by, for example, Greene & Lada (1996) to estimate the NIR veiling in T Tauri stars, however strong CO absorption features can arise in the disk photosphere as well as in the stellar photosphere (Calvet et

Send offprint requests to: D.F.M. Folha

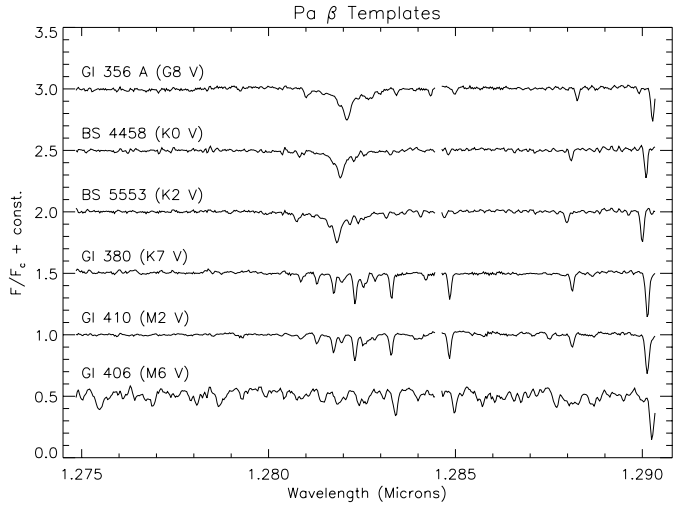

Fig. 1. Paβ region (J-band) template stars. Note that due to different stellar radial velocities the photospheric lines appear shifted from one star relative to another. The spectra are normalized to the continuum and shifted vertically for clarity. See also Fig. 4

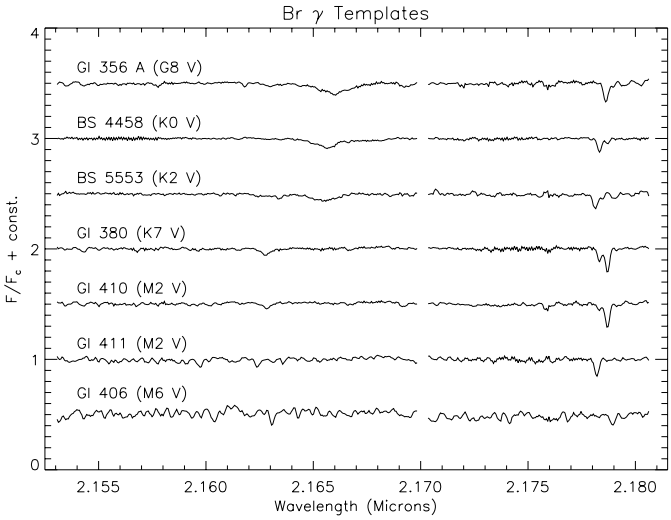

Fig. 2. Brγ region (K-band) template stars. Note that due to different stellar radial velocities the photospheric lines appear shifted from one star relative to another. The spectra are normalized to the continuum and shifted vertically for clarity. See also Fig. 4

al. 1997), implying that those absorptions are difficult to use to determine any NIR continuum veiling.

NIR high resolution spectroscopy allows one to observe the photospheric absorption lines of TTS present on this spectral region and determine the veiling. The strength of the NIR veiling can then be studied and interpreted.

We present an observational study of the veiling in the J and K wavebands for a sample of TTS, mostly from the Taurus-Auriga complex. The observations and data reduction are described in Sect. 2 and the method used to determine the veiling is presented in Sect. 3. The choice of template stars is discussed in Sect. 4, results are presented in Sect. 5, and compared with other data in Sect. 6. The discussion is in Sect. 7 and conclusions are presented in Sect. 8.

2. Observations and data reduction

The observations were carried out at the United Kingdom Infrared Telescope (UKIRT) between 15–17 December 1995 (UT) using the Cooled Grating Spectrometer No. 4 (CGS4) with the echelle grating, 150 mm focal length camera and 256×256 pixel SBRC InSb detector. Spectra centered at Paβ (1.28215 μm) were obtained for all TTS in Tables 1, and 2 and centered at Brγ (2.16611 μm) for all CTTS in Table 3 plus the WTTS Hubble 4. The spectral range covered is ~ 0.0154 μm around Paβ and ~ 0.0274 μm around Brγ. All observed spectra were sampled twice per resolution element ($\mathrm{R} = 20,500$). The slit size used was $1''0.2 \times 90''$ and the pixel size was $1''.2$ in the dispersion direction and $1''.8$ and $1''.7$ in the spatial direction, respectively for the Paβ and Brγ wavelength regions. The slit position was E-W at all times. Flat field frames were obtained and standard stars were observed for correction of atmospheric transmission and instrumental response. For more details on the observational procedures and observing logs refer to Folha (1998). Data reduction followed the general procedure described by Puxley et al. (1992) using CGS4DR, Figaro and IDL routines written specifically for this work. Spectral images were masked to avoid bad pixels and vignetted areas of the detector, de-biased and flat-fielded. Sky subtraction was achieved by subtracting sky frames from object frames. The spectra were optimally extracted using Figaro's implementation of the algorithm developed by Horne (1986) and, when needed, de-rippled using *deripple_spectrum* in CGS4DR. CVF fringing affected spectra in the Brγ window and the pattern was removed by filtering the spectra using standard Figaro tasks. Wavelength calibration used OH airglow emission lines and telluric absorption lines. The uncertainty in the wavelength calibration is 6–8 $\mathrm{km\,s^{-1}}$ at Paβ and 14–17 $\mathrm{km\,s^{-1}}$ at Brγ. The spectra have not been corrected for the stellar radial velocities. Thus the same absorption features do not quite appear at the same wavelength in successive frames of Figs. 1–5, which show our high resolution spectra. Atmospheric transmission and instrumental response was corrected by dividing the spectra of the target stars by the spectrum of one of the standard stars and multiplying by a black body spectrum of the appropriate effective temperature. Finally the continuum was normalized to unity by dividing by a cubic spline fit. For more details refer to Folha (1998).

A range of Main Sequence dwarfs were observed as template stars (the necessity of this will become clear in Sect. 3) at Paβ and at Brγ. These stars are: Gl 356 A (G8V), BS 4458 (K0V), BS 5553 (K2V), Gl 380 (K7V), Gl 410 (M2V), Gl 411 (M2V) and Gl 406 (M6V). Their Paβ and Brγ spectra are shown in Figs. 1 and 2 respectively.

The identification of photospheric features is in Fig. 3, where the K7V template star Gl 380 is shown together with the Paβ spectrum of AA Tau and the Brγ spectrum of GG Tau, two TTS. The photospheric lines are: at Paβ from left to right – Fe 7806.01 $\mathrm{cm^{-1}}$, Ti 7803.36 $\mathrm{cm^{-1}}$, Ca 7800.59 $\mathrm{cm^{-1}}$, Ti 7797.16 $\mathrm{cm^{-1}}$, Ti 7791.23 $\mathrm{cm^{-1}}$,

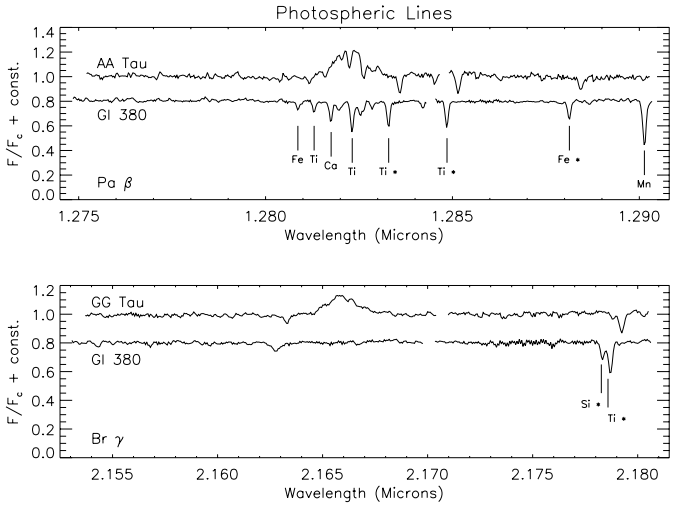

Fig. 3. *Top panel:* Paβ spectrum of AA Tau and Gl 380 (K7 V). *Bottom panel:* Brγ spectrum of GG Tau and Gl 380 (K7 V). See text for wavenumber of the photospheric lines. The photospheric lines labelled with an asterisk were used to determine the veiling. Due to different stellar radial velocities the photospheric lines appear shifted from one star relative to another. Spectra are normalized to the continuum and shifted vertically for clarity.

Ti 7781.77 cm^{-1}, Fe 7761.99 cm^{-1}, Mn 7749.92 cm^{-1}; and at Brγ – Si 4590.17 cm^{-1}, Ti 4589.50 cm^{-1} (vacuum wavenumbers). Of these Ti 7791.23 cm^{-1}, Ti 7781.77 cm^{-1}, Fe 7761.99 cm^{-1}, Si 4590.17 cm^{-1} and Ti 4589.50 cm^{-1} are the only ones used to determine the veiling. Line identification was done using the Near Infrared Solar Atlas of Livingston & Wallace (1991).

Fig. 4 shows the J and K-band spectra of the TTS. The wavelength ranges shown in Fig. 4 correspond only to the range where the photospheric lines used for veiling determination (see Sect. 3) are present.

3. Method

3.1. General

The veiling can be measured by comparing the spectrum of the veiled star with that of a template star of the appropriate spectral type, chosen such that its spectrum accurately represents the (unveiled) photospheric spectrum of veiled star. Hereafter, the veiling measured in J-band near Paβ will be referred to by $r_{\rm J}$ and that measured in K-band near Brγ by $r_{\rm K}$. The choice of appropriate template stars is discussed in Sect. 4 below.

A number of different methods to determine the veiling in a TTS have been discussed in the literature. The veiling can be determined by comparing the equivalent widths of a set of photospheric lines in the spectrum of the TTS and in that of a template star of the appropriate spectral type whose spectrum has been broadened (numerically) to the same $v \sin i$ as the TTS. However, this method works better when there is a range of photospheric lines with different excitation potentials (Basri & Batalha 1990), which is not the case for our data. Basri & Bertout (1989) use an auto-correlation method, Hartigan et al. (1989) use a χ^2-algorithm to fit pixel by pixel the observed spectrum with that of a template star (broadened for rotation) plus a featureless continuum, Guenther & Hessman (1993) use a cross-correlation method based on a technique discussed by Tonry & Davis (1979), where the cross-correlation function between the TTS spectrum and that of a template star (broadened for rotation) is computed along with the auto correlation function of the spectrum of the template star.

3.2. Application at J

Given the available data set, the latter method was selected, for the J-band, to compute the amount of veiling in the TTS for which the photospheric spectrum could be identified. Following Tonry & Davis (1979), the data was filtered before computing the cross- and auto-correlation functions, in order to remove low frequency spectral variations as well as high frequency components due to noise, as this greatly decreases the possible bias due to bad noise estimates (see Chelli 1999). The veiling is determined by computing the ratio of the peak of the auto-correlation function to the peak of the cross-correlation function and subtracting unity. The uncertainty in the veiling comes from the uncertainties of the peaks of the auto and cross-correlation functions[1]. These were estimated from the root mean square of the antisymmetric component of these functions (Tonry & Davis 1979). The method used is, in principle, equivalent to the point to point method used by Hartigan et al. (1989). Problems of biases in the results due to bad noise estimates and spectral mismatches are thoroughly analyzed in Chelli (1999).

A section of the spectrum containing only continuum and photospheric lines was cross correlated with the corresponding wavelength region of the chosen template star (broadened for rotation). For the J-band data, the wavelength region chosen was ~ 1.2830–$1.2890\,\mu$m to avoid Paβ emission/absorption around $1.282\,\mu$m. The three photospheric features are Ti 7791.23 cm^{-1}, Ti 7781.77 cm^{-1} and Fe 7761.99 cm^{-1}, and are marked at the top of each panel of Fig. 4. At times, the former is affected by a redshifted absorption feature in Paβ. For those cases only Ti 7781.77 cm^{-1} and Fe 7761.99 cm^{-1} were used to determine the veiling.

To test the cross-correlation method for the veiling at J, spectra of template stars were veiled by a known amount and different levels of noise were added. The method was then applied to check whether the correct amount of veiling was recovered. Fig. 5 shows the spectrum of the K7V template star Gl 380 artificially veiled and with a decreased signal-to-noise ratio, as well as the original unveiled observed spectrum. In each of the panels the signal-to-noise ratio of the veiled spectrum decreases towards the bottom (at 50:1, 20:1 and 10:1 respectively). Spectra in the top panel have a veiling of 0.5, and in the lower panel 1.5. Applying the cross-correlation method between $\sim 1.2830\,\mu$m to $\sim 1.2890\,\mu$m (using Gl 380 as the template)

[1] Both the cross-correlation function and the auto-correlation function are non normalized.

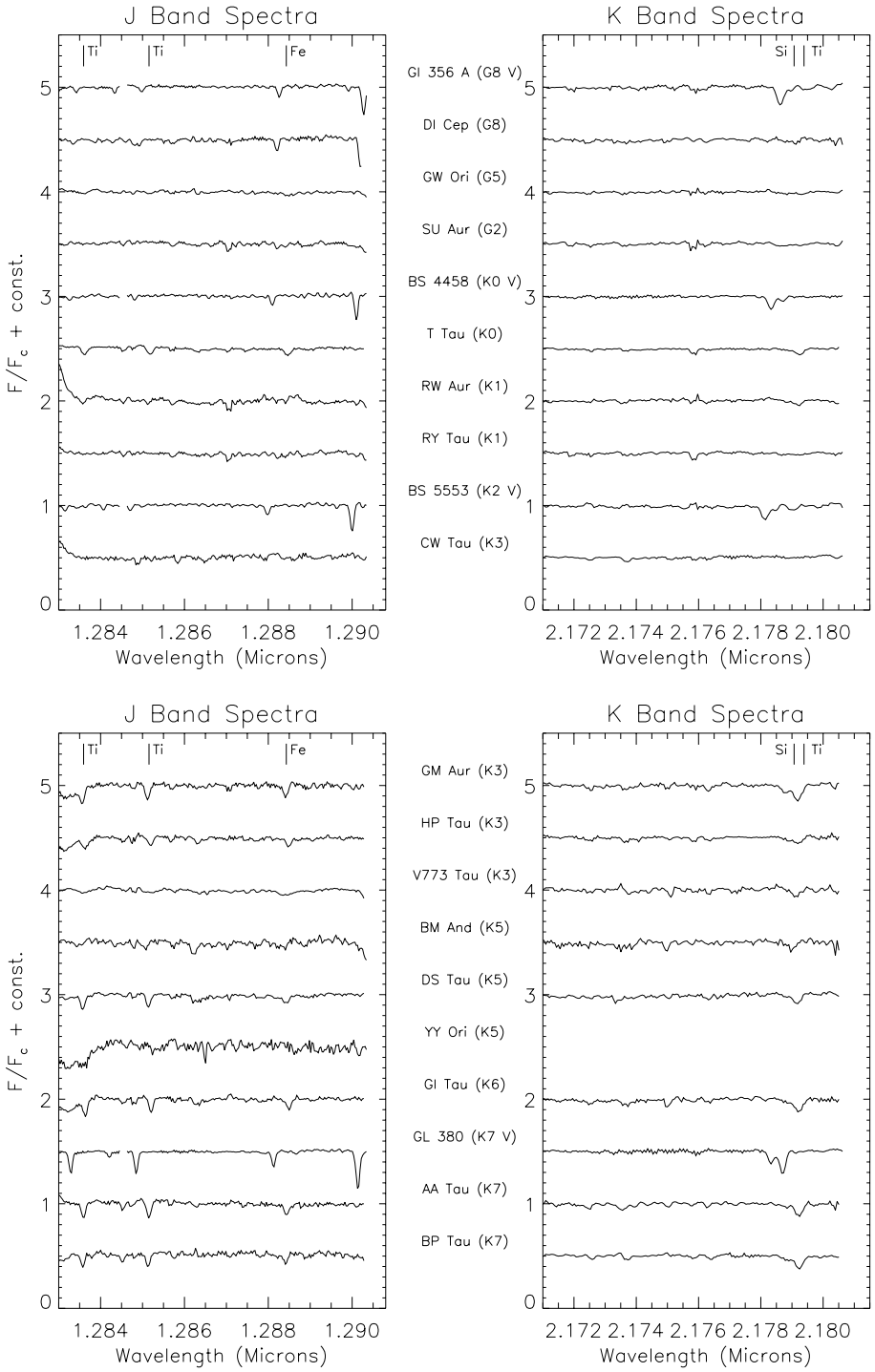

Fig. 4. J-band (panels on the left) and K-band (panels on the right) TTS' and templates' spectra, containing the photospheric lines used to determine the veiling. Stars are ordered by spectral type. The photospheric lines used are marked at the top of each panel. Note that due to different stellar radial velocities the photospheric lines appear shifted from one star relative to another. The spectra are normalized to the continuum and shifted vertically for clarity. Figure continued.

the following veilings were obtained: top panel top to bottom spectra 0.49 ± 0.04, 0.53 ± 0.10 and 0.46 ± 0.15; lower panel top to bottom spectra 1.57 ± 0.09, 1.74 ± 0.25 and 1.25 ± 0.44. Comparing these with the known veiling added one sees good agreement within the uncertainties. However in this test there is no mismatch between the spectral type of the object and the template, and any such mismatches will introduce added uncertainty. The choice of template stars and spectral mismatches are discussed in Sect. 4. All tests performed showed that this is a reliable method to compute the amount of veiling from the spectrum of a T Tauri star using the data set analyzed here.

3.3. Application at K

The cross-correlation method could not determine the veiling in the Brγ wavelength region. This is because only two photospheric lines are present for the veiling computation (Ti 4589.50 cm^{-1} and Si 4590.17 cm^{-1}), they are somewhat

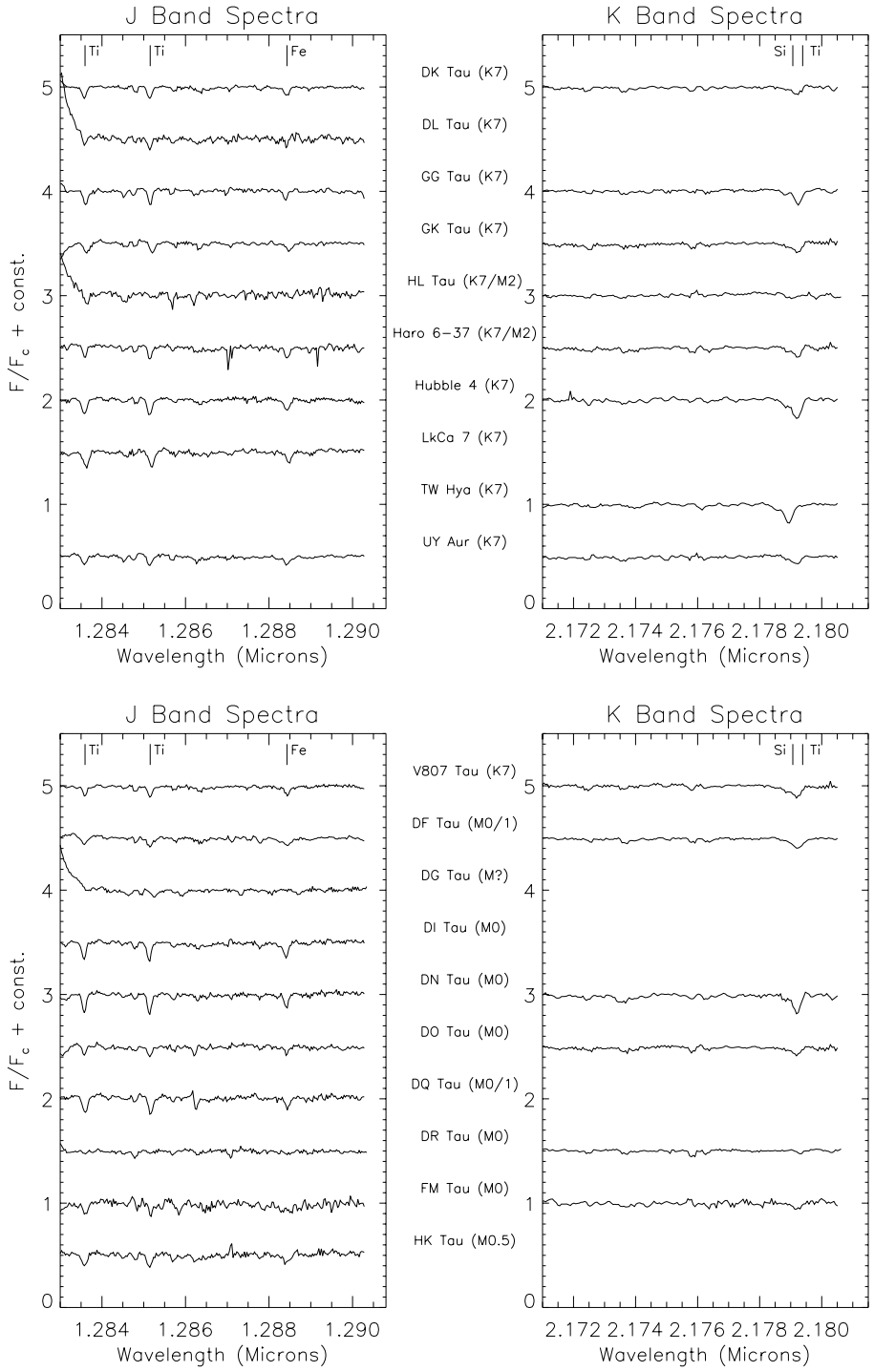

Fig. 4. (continued)

blended (see Fig. 3) and the signal-to-noise ratio is, in general, lower than at Paβ wavelengths. Nevertheless, the K-band veiling was computed, although by a different, less precise, method. After deciding on the correct template star (see Sect. 4), its spectrum was broadened to account for rotation and then veiled by a known amount and the result subtracted from the T Tauri star spectrum. This procedure was carried out starting from a veiling of zero up to an amount clearly not consistent with the data, in steps of 0.1. A range of values consistent with the data was chosen, as judged by eye. The veiling was taken to be the mean of the above values with an estimate for the error being the difference between the mean and the most extreme value.

Our method assumes that there is a constant veiling across approximately 50 Å in the J-band and 20 Å in the K-band (where the photospheric lines we use to determine the veiling are present), but not from one band to the next. If the photospheric lines are instead filled in by line emission, or other effects spe-

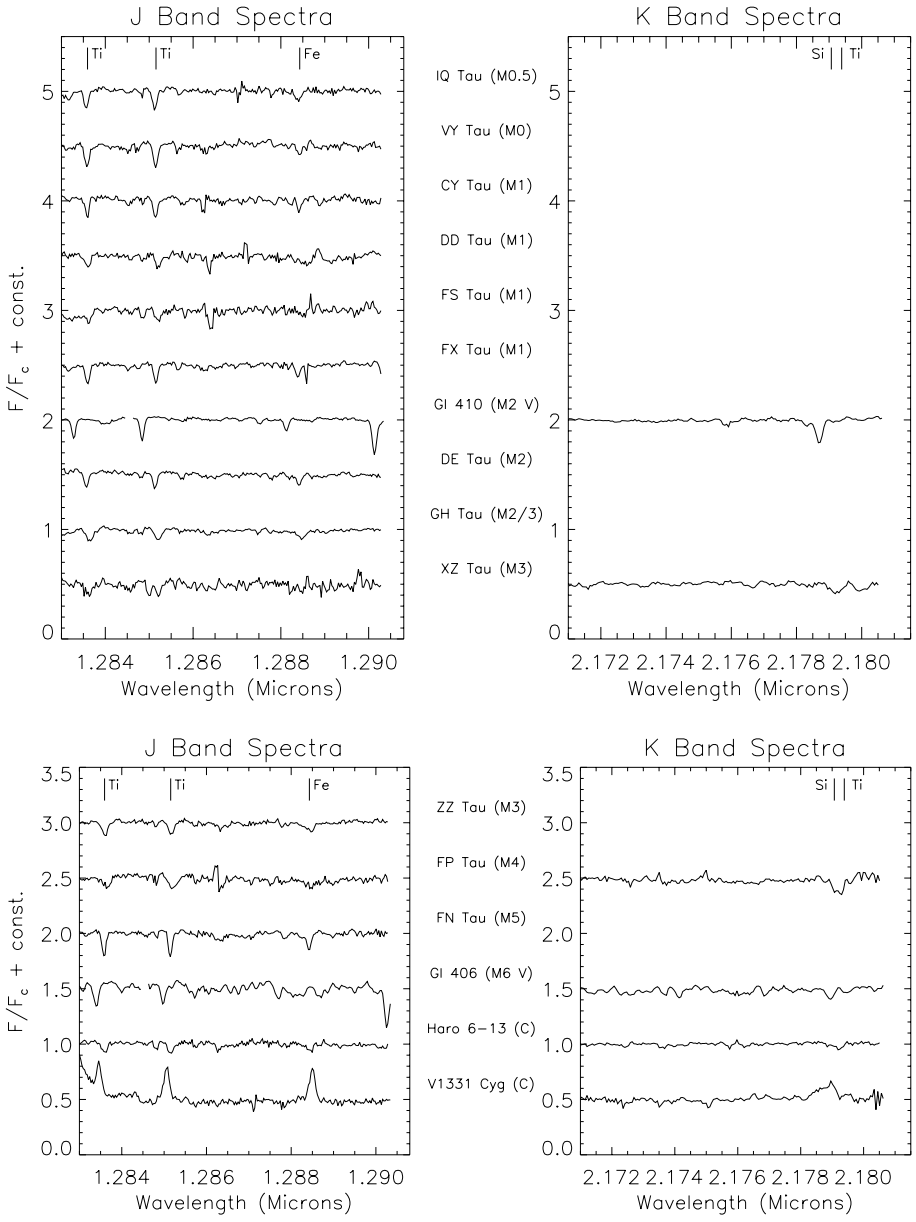

Fig. 4. (continued)

cific to their individual wavelengths, our method may not be appropriate.

4. Choice of Template Star

The template star to use in the veiling calculation was, with a very few exceptions discussed below, decided on the basis of the optically derived spectral type of the TTS in the Herbig-Bell Catalogue (Herbig & Bell 1988, hereafter HBC). Most of the stars for which photospheric lines were identified have spectral types between K7V and M2V (26 out of 38 stars with photospheric lines in the Paβ region). For these stars, either K7V or M2V templates were used.

For the four stars with spectral type later than M2V (up to M5V) the M2V template was used as the NIR spectra of these stars (FN Tau, FP Tau, GH Tau (a binary) and ZZ Tau (a binary) resemble the M2V template more than the M6V template, even in the case of FN Tau, a single M5V star.

Of the eight stars with spectral types earlier than K7V three are within two subclasses of K7V and lacking a better template Gl 380 (K7V) was used. For DI Cep, a G8V star, Gl 356 A, a G8V template was used.

The veiling in the CTTS Haro 6-13, classified as a 'continuum' star in the optical, was computed using the K7V template. This is based on the K-band spectrum of Haro 6-13 having the Ti line deeper than the Si. From our template stars, the ones with this characteristic are those with spectral types K7V and M2V. The photospheric lines in the J-band spectrum of Haro 6-13 are deeper than those in the K2, K0 and G8 dwarves, but not as deep as in the K7V or M2V stars. Being the star with earlier spectral type available in our set of template stars with a spectrum compatible with that of Haro 6-13, the K7V was preferred. Using

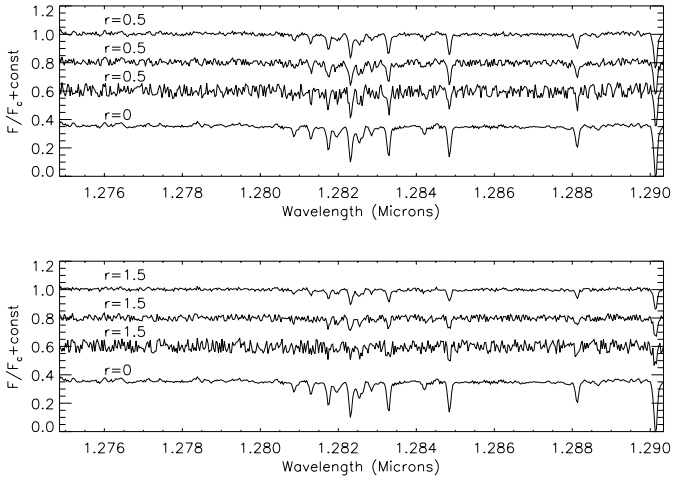

Fig. 5. *Top panel:* Paβ spectrum of Gl 380 as observed (r=0); veiled (r=0.5) and noisier (by 2%, 5% and 10% top down). *Bottom panel:* Same as above for veiling r=1.5. Spectra are shifted vertically for clarity.

either the K7V or the M2V as templates would give essentially the same result for the veiling determination (see Sect. 4.2).

A K7V template was used in the remaining four TTS, HP Tau (a binary), V773 Tau (a binary) and GM Aur (all are K3V stars) and T Tau (K0V, a binary), giving the largest mismatches between the spectral type attributed from optical spectroscopy and the type of the template star used to compute the veiling. K7V was adopted because in the K-band spectrum of all four stars, the relative intensity of the two photospheric lines near 2.179 μm resemble a K7V star more than K0 or even K2 dwarfs, where the Si line should be the stronger of the two. Also, the photospheric lines seen near Paβ are deeper than the corresponding ones in the K0V and K2V templates, implying a later spectral type. On this basis, Gl 380 (K7V) was used as template.

The presence of redder unresolved (within the width of CGS4's slit) companions might be a reason for this possible discrepancy in spectral types. This is considered in Sect. 4.1. A different explanation is that rather than seeing the stellar photosphere one might also be seeing a contribution from the 'photosphere' of the circumstellar disk, or from cool starspots on the surface, or from the accretion column or shock. These possibilities are implicitly addressed in Sect. 7.

From the two M2V stars observed at Brγ, Gl 410 was chosen as a M2V template star. The two stars have slightly different photospheric spectra, as can be seen from Fig. 2. The Wallace & Hinkle (1996) atlas of cool stars in the K-band also presents the spectrum of Gl 411 which looks very similar to the spectrum presented here. These authors express their surprise at the fact that the spectrum of Gl 411 is not as similar as expected to the spectrum of the K7V star they observed (61 Cyg B), given the similar spectral types of the two stars, probably as Gl 411 is deficient in metals (Wallace & Hinkle 1996). Given that the K band spectrum of Gl 410 presented here is, as expected, similar to that of the K7V star observed (Gl 380) and also since the signal-to-noise ratio in its spectrum is slightly higher than that in Gl 411's spectrum we chose Gl 410 as a M2V template for this wavelength region.

Three Weak Line T Tauri stars (WTTS) were observed. In principle they could have been used as template stars for the determination of the veiling in the Classical T Tauri stars (CTTS). One would expect their veiling to be zero, since they are taken to be non accreting TTS. Indeed, the veiling of all WTTS observed are compatible with zero, however, the values found are, with the exception of the K veiling of Hubble 4, not quite zero (see Table 1).

Because they are single, and had higher signal to noise spectra, the main sequence stars observed were preferred over the WTTS as templates.

Tables 2 and 3 lists the optical spectral types (from HBC) of the TTS for which NIR veiling was determined. The spectral types of the templates used to derive the NIR veiling are also listed there.

4.1. Binary/multiple systems in the sample

Contribution to the spectrum from an unresolved binary companion in the CGS4 slit may affect the apparent spectral type of the star, or might be mistaken for veiling local to the TTS. Lists of known binary TTS in Taurus were therefore consulted (Ghez et al. 1991; Ghez et al. 1993; Leinert et al. 1993; Richichi et al. 1994; Mathieu 1994; Simon et al. 1995; Ghez et al. 1997) to check if any of our sample are known to be binaries that would be unresolved to our $1.2''$ wide slit. Binaries are noted 'b' in Tables 1 to 3.

T Tau is a binary system (separation $\sim 0.5''$) with a cool IR companion star (Ghez et al. 1991) which might be contaminating the NIR spectrum and therefore making it look like that of a later spectral type object. HP Tau is a binary system with a separation of $\sim 0.2''$ which might make the NIR spectrum of HP Tau look like that of a star with a later spectral type. V773 Tau is a multiple system with an unresolved component that contributes considerably to the total spectral energy distribution (Ghez et al. 1997) which is likely to be of K5V spectral type.

As noted above, T Tau, HP Tau and V773 Tau have NIR spectra that look more like those of a K7V star than like those of the earlier type stars (K3V/K0V) that their optical spectra reveal. The presence of cooler companion stars in the CGS4 slit might be the cause of such discrepancies between optical and near IR spectral types. DF Tau, DI Tau, FS Tau,GG Tau, GH Tau, LkCa7, UY Aur, V807 Tau, VY Tau and ZZ Tau are all binary stars with separation less than $2''$ (Mathieu 1994). Despite that, the near IR spectrum of these stars corresponds to the spectral types expected from optical observations.

4.2. Spectral type mismatch

The main source of uncertainty in the computation of the NIR veiling for a given TTS is the choice of the template star used. The way in which this choice was made was described above.

The stars for which the veiling determination should be least affected by a mismatch in spectral type are the K7V to M2V stars

Table 1. Veilings for the Weak Line T Tauri stars (WTTS). Column 1 star name, Column 2 spectral type from the Herbig-Bell Catalogue (Herbig & Bell 1988), Column 3 indicates if a binary/multiple system, Column 4 $r_{\rm J}$, veiling near Paβ, Column 5 spectral type of template star used, Column 6 $r_{\rm K}$, veiling at Brγ, and Column 7 spectral type of template star. '–' means the star was not observed.

Star	Sp. Type (HBC)	Binary	$r_{\rm J}$ Veiling Paβ	Sp. Type (Paβ Template)	$r_{\rm K}$ Veiling Brγ	Sp. Type (Brγ Template)
DI Tau	M0	b	0.10±0.11	K7	–	–
Hubble 4	K7		0.17±0.10	K7	0.0±0.1	K7
Lk Ca 7	K7	b	0.17±0.09	K7	–	–

in the sample. Why? On the one hand inspecting the spectra of the TTS with spectral types K7V to M2V one sees that they are as expected for a star of those spectral types, while the same is not true for some stars of earlier spectral type (e.g. GM Aur, HP Tau and T Tau). The 'J veiling' of the K7V template determined with the M2V template is $r_{\rm J} = 0.1 \pm 0.1$, consistent with zero (but positive). A spectral type mismatch between the TTS and the template stars of 2 to 3 subclasses around M0V does not seem to influence the J veiling beyond the quoted uncertainties. Larger mismatches can lead to an erroneous J veiling. As an example, if the K7V star is used to determine the 'J veiling' of the K0V star, the value is $r_{\rm J} = 3.0 \pm 0.8$. This is due to the fact that the photospheric lines used here to measure the veiling are not as deep in a K0V as in a K7V star.

In the K-band the veiling of Gl 380 (K7V) determined with Gl 410 (M2V) is $r_{\rm K} = 0.0 \pm 0.05$. Therefore, the veiling of the TTS determined with either template is the same. Since early and late K spectral types have basically the opposite ratio of the photospheric lines Si 4590.17 cm^{-1} and Ti 4589.50 cm^{-1}, it is almost impossible to misclassify a TTS by so many spectral classes based on spectra in this wavelength range.

For the spectral type range discussed in this work (late G to early M dwarves) if the spectral type of the template star used is later than that of the TTS, the veiling of the latter is overestimated. In this work, this mismatch is seldom larger than two subclasses.

5. Results

5.1. Weak line T Tauri stars

Table 1 show the results obtained for the WTTS. The $r_{\rm J}$ of DI Tau, Hubble 4 and Lk Ca 7 and the $r_{\rm K}$ of Hubble 4 are compatible with zero, as expected for WTTS.

Hubble 4 and LkCa 7 have $r_{\rm J} = 0.17$, while one would expect to find a zero. If this is a systematic effect and if $r_{\rm J}$ is really zero for these WTTS then the $r_{\rm J}$s for the CTTS might be biased towards larger values of the veiling with a relative bias of ~ 0.2 (see Eq. 12 in Chelli 1999).

Such results might arise if the photospheric spectrum of TTS is not well represented by that of a main-sequence dwarf star. Indeed, typical TTS should have larger radii than dwarf main-sequence stars and therefore some characteristics of giant main-sequence stars might occur in their photospheric spectra. However, Meyer (1996) found with H band observations that TTS appear to have surface gravities closer to dwarf stars than giant stars but with some characteristics of the latter.

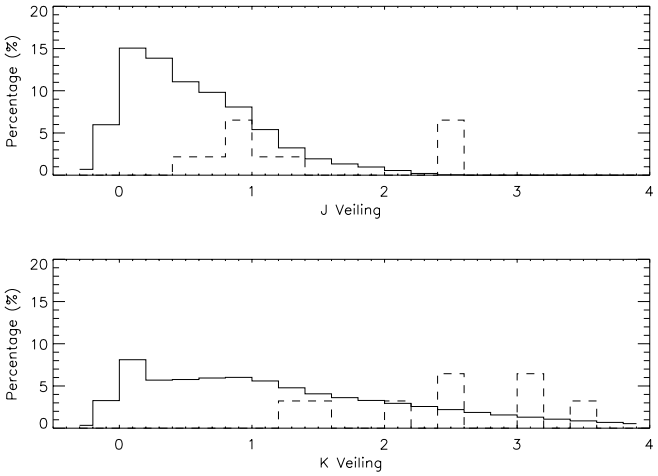

Fig. 6. *Top panel:* the solid line represents the distribution of the veiling at J for stars with veiling determined. The dashed line represents the contribution to the histogram of the stars for which only lower limits were obtained; *Bottom panel:* Same as top panel but for K veiling.

5.2. Classical T Tauri stars: veiling

The results for the J and K bands are presented in Tables 2 and 3 respectively. The stars are divided into five groups: those having a veiling compatible with zero, those having a veiling for which zero can be excluded at the 1σ level, at the 2σ level and at the 3σ level, and those with lower limit only.

Photospheric lines are present in the spectrum of 73% of the CTTS observed at J. Of the 33 CTTS for which the J veiling was measured, 8 have values compatible with $r_{\rm J} = 0$. Of the remaining 25 $r_{\rm J} = 0$ can be excluded at the 1σ level in 3 cases, at the 2σ level in 10 cases, and the 3σ level in 12 cases (mean $r_{\rm J} = 0.97$).

Photospheric lines are present in the spectrum of 71% of the CTTS observed at K. Of the 22 CTTS with $r_{\rm K}$ measured, 3 have values compatible with $r_{\rm K} = 0$. Of the remaining 19 $r_{\rm K} = 0$ can be excluded at the 1σ level in 2 CTTS, at the 2σ level in 10 CTTS, and at the 3σ level in 7 CTTS (mean $r_{\rm K} = 1.76$).

The histograms of $r_{\rm J}$ and $r_{\rm K}$ for the stars for which the veiling could be determined are shown in Fig. 6 as a solid line. To take into account the uncertainties in our veilings we show histograms in which each veiling value has been divided over a number of bins as appropriate for a Gaussian distribution of uncertainties. This procedure also allows use of finer bins with significant number of counts in them. Further details are given in Appendix A.

Table 2. J veiling ($r_{\rm J}$) for the CTTS. Stars are divided into 5 groups: those with $r_{\rm J}$ compatible with zero, those with $r_{\rm J} = 0$ excluded at the 1σ level, 2σ level, 3σ level and lower limits. Column 1 star name, Column 2 spectral type from HBC, Column 3 'b' a binary/multiple system, Column 4 $r_{\rm J}$ and Column 5 template's spectral type.

Star	Sp. Type (HBC)	Binary	$r_{\rm J}$ Veiling Paβ	Template Sp. Type
Compatible with $r_{\rm J} = 0$				
DI Cep	G8		0.02±0.15	G8
DN Tau	M0		0.08±0.10	K7
DQ Tau	M0/1		0.15±0.19	K7
FN Tau	M5		-0.05±0.12	M2
FP Tau	M4		0.21±0.23	M2
GH Tau	M2/3	b	0.11±0.18	M2
IQ Tau	M0.5		0.12±0.12	K7
VY Tau	M0	b	-0.04±0.09	K7
$r_{\rm J} = 0$ excluded at the 1–2σ level.				
CY Tau	M1		0.17±0.10	M2
FM Tau	M0		1.02±0.52	K7
GM Aur	K3		0.30±0.16	K7
$r_{\rm J} = 0$ excluded at the 2–3σ level.				
AA Tau	K7		0.21±0.08	K7
DE Tau	M2		0.41±0.15	M2
DF Tau	M0/1	b	0.95±0.34	K7
FX Tau	M1		0.35±0.16	M2
GG Tau	K7	b	0.38±0.14	K7
GI Tau	K6		0.40±0.17	K7
HK Tau	M0.5		0.43±0.21	K7
HP Tau	K3	b	1.06±0.36	K7
Haro 6-37	K7/M0		0.54±0.25	K7
ZZ Tau	M3	b	0.60±0.22	M2
$r_{\rm J} = 0$ excluded at the $\geq 3\sigma$ level.				
BP Tau	K7		0.52±0.14	K7
DD Tau	M1	b	0.99±0.21	M2
DK Tau	K7	b	0.72±0.20	K7
DO Tau	M0		1.07±0.28	K7
DS Tau	K5		0.57±0.19	K7
FS Tau	M1	b	1.86±0.26	M2
GK Tau	K7		0.72±0.22	K7
Haro 6-13	C		0.99±0.28	K7
T Tau	K0	b	0.78±0.15	K7
UY Aur	K7	b	0.84±0.20	K7
V773 Tau	K3	b	1.37±0.40	K7
V807 Tau	K7	b	1.20±0.33	K7
Lower limits to $r_{\rm J}$.				
BM And	K5		>1.4	K7
CW Tau	K3		>1.2	K2
DG Tau	M?		>2.5	M2
DL Tau	K7		>0.7	K7
DR Tau	M0		>2.5	K7
GW Ori	G5	b	>0.8	G8
HL Tau	K7/M2		>2.5	K7
RW Aur	K1		>0.5	K2
RY Tau	K1		>0.8	K2
SU Aur	G2		high	–
XZ Tau	M3		>0.8	M2
YY Ori	K5		>1	K7

Table 3. Same as Table 2 for $r_{\rm K}$

Star	Sp. Type (HBC)	Binary	$r_{\rm K}$ Veiling Brγ	Template Sp. Type
Compatible with $r_{\rm K} = 0$				
DN Tau	M0		0.1±0.1	K7
FP Tau	M4		0.4±0.4	M2
TW Hya	K7		0.1±0.1	K7
$r_{\rm K} = 0$ excluded at the 1–2σ level.				
FM Tau	M0		3.3±1.7	K7
GM Aur	K3		0.3±0.2	K7
$r_{\rm K} = 0$ excluded at the 2–3σ level.				
AA Tau	K7		0.8±0.4	K7
BM And	K5		1.4±0.5	K7
BP Tau	K7		0.8±0.3	K7
DO Tau	M0		1.8±0.7	K7
DS Tau	K5		1.1±0.5	K7
GG Tau	K7	b	0.4±0.2	K7
GI Tau	K6		0.6±0.3	K7
HP Tau	K3	b	2.2±0.8	K7
Haro 6-37	K7/M0		2.0±1.0	K7
V807 Tau	K7	b	0.8±0.4	K7
$r_{\rm K} = 0$ excluded at the $\geq 3\sigma$ level.				
DF Tau	M0/1	b	0.9±0.3	K7
DK Tau	K7	b	1.8±0.6	K7
GK Tau	K7		1.1±0.3	K7
Haro 6-13	C		2.7±0.9	K7
T Tau	K0	b	2.5±0.7	K7
UY Aur	K7	b	1.8±0.5	K7
V773 Tau	K3	b	1.5±0.5	K7
Lower limit to $r_{\rm K}$.				
CW Tau	K3		>3.5	K2
DI Cep	G8		>2	G8
DR Tau	M0		>3	K7
GW Ori	G5	b	>2.5	G8
HL Tau	K7/M2		>3	K7
RW Aur	K1		>1.5	K2
RY Tau	K1		>2.5	K2
SU Aur	G2		high	–
XZ Tau	M3		>1.2	M2

The mean values of the distributions represented as solid lines in Fig. 6 are $\langle r_{\rm J} \rangle = 0.57$ and $\langle r_{\rm K} \rangle = 1.29$. Considering only stars with veilings determined to better than 3σ these means are $\langle r_{\rm J} \rangle = 0.97$ and $\langle r_{\rm K} \rangle = 1.76$. Although most stars have relatively low J and K veiling, the distributions clearly have an extended tail towards higher values of veiling.

Excluding the stars in known binary/multiple systems does not significantly change the shape of the distributions, indicating that the inclusion of some binaries is not significantly affecting our results.

5.3. Classical T Tauri stars: veiling lower limits

In 27% of the CTTS observed at J (12 out 45) and in 29% of the CTTS observed at K (9 out of 31) photospheric lines are not identified. CW Tau, DR Tau, GW Ori, HL Tau, RW Aur,

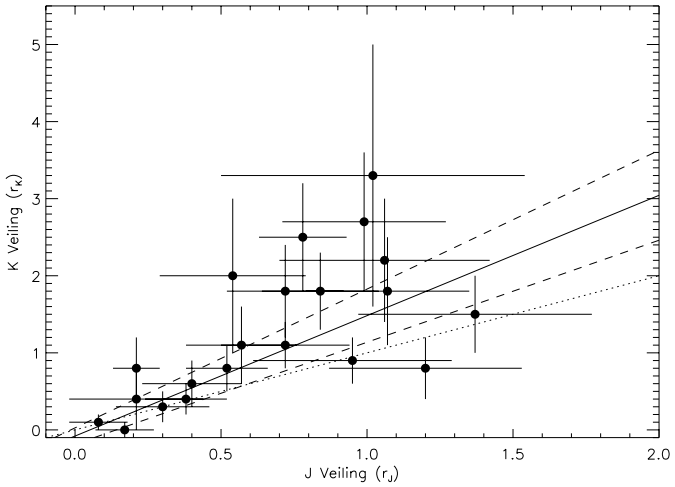

Fig. 7. J veiling ($r_{\rm J}$) vs. K veiling ($r_{\rm K}$) for the stars with the two measurements. The dotted line is $r_{\rm K} = r_{\rm J}$.
The solid line is the best straight line fit weighted by the uncertainties in $r_{\rm J}$ and in $r_{\rm K}$ ($r_{\rm K} = (-0.1 \pm 0.1) + (1.56 \pm 0.24) r_{\rm J}$). The dashed lines are the two extremes that result from the uncertainties.

RY Tau, SU Aur and XZ Tau show no photospheric lines either at J or at K; DG Tau, DL Tau and YY Ori show no photospheric lines at J only, but were not observed at K.

For BM And, one cannot say that photospheric features are not present since the blue wing of Mn 7749.92 cm^{-1} is clearly seen at the red edge of the spectrum. However, the red wing of the line lies beyond the observed wavelength range and only a lower limit on $r_{\rm J}$ could be obtained from the (lack of) Ti & Fe lines.

No appropriate template star was observed to allow a similar measurement for SU Aur, a G2 star. Given its spectral type from optical observations, SU Aur should have a clearly visible Si 4590.17 cm^{-1} absorption line in the K-band spectrum. The Si line is not identified though, implying high K band veiling for this star. It should be noted that the optical veiling of SU Aur is zero (Basri & Batalha 1990).

There are two possible explanations for our lack of any detections of photospheric absorption lines in these objects. On the one hand the photospheric lines can be masked under a noisy spectrum. On the other hand a TTS might be so veiled that the photospheric lines cannot be identified.

For the above stars, with the exception of SU Aur, lower limits on the J and K veiling were obtained by veiling the spectrum of an appropriate template star up to a level such that the depth of the photospheric absorption features became comparable to the fluctuations on the TTS's spectrum. The results are presented in Tables 2 and 3. The mean of the lower limits in the J-band is $\langle r_{\rm J} \rangle > 1.34$, and in the K-band is $\langle r_{\rm K} \rangle > 2.4$.

The lowest lower limits occur for early type stars, like GW Ori, RW Aur and RY Tau, for which the photospheric lines in the template stars are not very strong, making the veiling measurements difficult (note that the strong Mn feature is, for the TTS, out of the observed wavelength region due to their radial velocities) or for stars with low signal-to-noise ratio, like XZ Tau. The distribution of the lower limits on the veiling are plotted in Fig. 6 using dashed lines. As can be seen, the lower limits tend to be relatively high, implying that the true distributions are actually enhanced for higher values of veiling when compared to those represented by a solid line in Fig. 6.

The non-identification of photospheric features in the spectra of some TTS tends therefore also to reflect high veiling for the NIR wavelength region.

A CTTS observed, but not included in the statistics above is V1331 Cyg, whose photospheric lines we find to be in emission (see last spectrum in Fig. 4) making the determination of the veiling impossible. Its spectral type is unknown. This star also displays photospheric lines in emission at optical wavelengths (Gameiro, private communication).

5.4. Effect of magnetic fields

Magnetic fields tend to broaden photospheric lines and hence increase their equivalent width, which is proportional to the magnetic sensitivity $\lambda^2 {\rm g}_{\rm eff}$, where λ is the wavelength of the line and ${\rm g}_{\rm eff}$ is the effective Landé factor (Guenther et al. 1998). As discussed by Guenther et al. (1998), such an increase in the equivalent width might result in an underestimation of the veiling for TTS if the Landé factor of the photospheric lines used for the veiling is not zero. The Landé factors for the photospheric lines used for the veiling determination in this work are: at J, 0.67 for Ti 7791.23 cm^{-1}, 1.08 for Ti 7781.77 cm^{-1} and 1.50 for Fe 7761.99 cm^{-1}; at K 1.25 for Ti 4589.50 cm^{-1} (Ruedi et al. 1995). Therefore, the results presented above for the veiling underestimate the true veiling if there are magnetic fields, as expected.

5.5. Relationships between $r_{\rm J}$ & $r_{\rm K}$

Fig. 7 plots $r_{\rm J}$ versus $r_{\rm K}$ for the stars that had the veiling determined at both wavelength regions. Despite the large uncertainties there is some correlation between $r_{\rm J}$ and $r_{\rm K}$. In Fig. 7 the dotted line is $r_{\rm K} = r_{\rm J}$. The best straight line fit to the data, weighted by the uncertainties on both axes, is $r_{\rm K} = (-0.1 \pm 0.1) + (1.56 \pm 0.24) r_{\rm J}$, which is the solid line in Fig. 7. The dashed lines are the two extremes that result from the uncertainties.

5.6. Section conclusion

We conclude that despite the uncertainties there is strong evidence (at above the 3σ level) for substantial veiling of the photospheric lines in 12 objects ($\langle r_{\rm J} \rangle = 0.97$) at J-band and in 7 objects ($\langle r_{\rm K} \rangle = 1.76$) at K-band, and of high veiling in objects for which we can only determine lower limits to r.

6. Comparison with other data

6.1. Comparison with other work

One does not find J-band spectroscopic veiling determinations for TTS in the literature. At a wavelength intermediate between

the J and K bands Meyer (1996) computed veiling at 1.62μm in the H-band for four CTTS and found relatively high values (e.g. 4 for DR Tau). Greene & Meyer (1995) and Casali & Eiroa (1996), observed excess K emission in Young Stellar Objects (including some TTS) from NIR intermediate spectral resolution spectroscopy. They find that the observed sources are affected by veiling emission from hot dust. Greene & Lada (1996) discuss these results and find that $r_{\rm K}$ depends on the SED; their Class III sources have $r_{\rm K} = 0.1 \pm 0.1$, Class II have $r_{\rm K} = 0.6 \pm 0.7$ and flat-spectrum sources have $r_{\rm K} = 1.9 \pm 0.7$. These results were obtained by combining spectroscopic and photometric data, with the assumption that $r_{\rm J} = 0$. CTTS correspond mostly to Class II sources, although some CTTS are flat-spectrum sources. The results presented here imply $\langle r_{\rm K} \rangle = 1.29$ (or considering only values of $r_{\rm K}$ determined to 3σ or better $\langle r_{\rm K} \rangle = 1.76$, or considering only lower limits $\langle r_{\rm K} \rangle > 2.4$) which are high compared to the value estimated for Class II by Greene & Lada (1996).

The $r_{\rm K}$ for the four CTTS in our sample that are flat-spectrum sources in Greene & Lada (1996) are, in general, consistent with the average $r_{\rm K}$ found by these authors for flat-spectrum sources. However, the values we determine tend to be systematically higher than the Greene & Lada average. The assumption that $r_{\rm J} = 0$ is crucial for the determination of $r_{\rm K}$ by those authors. If $r_{\rm J}$ has a mean value near $\langle r_{\rm J} \rangle = 0.57$, as we determine (over the whole sample), then using Eqs. 5 and 6 in Greene & Meyer (1995) one concludes that their mean $r_{\rm K}$ should be about 1.5, which is in tune with the measurements presented here, that give a mean $r_{\rm K}$ of 1.29.

To check consistency between the NIR veilings and photometric J-K colours of TTS, we determined the J-K colour corresponding to the J and K veilings, for stars common to our and Strom et al.'s (1989) samples, and for which the K7V template stars were used to compute the J and K veiling. The predicted J-K ignored reddening since the values for the visual extinction found in the literature vary so much that we chose not to correct for reddening. The large uncertainties in the veilings, especially at K, cause large uncertainties. Further our veilings and Strom et al.'s (1989) J-K colours are not simultaneous leading to another potential source of discrepancy (see Chelli et al. 1999). Our predicted (J-K) tends to be systematically smaller than the photometric observations. Accounting for extinction would tend to bring our predictions and the observations closer together. This comparison serves only to show that our veilings are not so large as to be inconsistent with observed photometric J-K colours.

Thus our results are consistent with other observations.

7. Discussion of veiling results

7.1. Colour temperature of veiling

The veilings presented here, in principle, allow one to estimate the J-K colour temperature, $T_{\rm veil}$, of the region producing this NIR veiling. Assuming that the excess flux that veils the stellar photosphere at these wavelengths is characterised by a black body of temperature $T_{\rm veil}$ one can use the values of $r_{\rm J}$ and $r_{\rm K}$ to compute the excess fluxes at J ($F_{\rm J}(excess)$) and at K ($F_{\rm K}(excess)$). A black body through these two points yields $T_{\rm veil}$. From the definition of veiling one sees that in order to compute $F_{\rm J}(excess)$ and $F_{\rm K}(excess)$ from $r_{\rm J}$ and $r_{\rm K}$ one needs the stellar flux at J and K respectively. Given that no flux calibration is available the stellar flux was estimated from a black body of temperature $T_{\rm eff} = 4000\,$K, corresponding roughly to stars of spectral type K7V/M0V, a typical stellar radius equal to the solar radius and a distance of 140 pc, appropriate for Taurus. This is a justifiable approximation, given the relatively large uncertainties in $r_{\rm J}$ and $r_{\rm K}$.

For the average values of $r_{\rm J}$ and $r_{\rm K}$ ($\langle r_{\rm J} \rangle = 0.57$ and $\langle r_{\rm K} \rangle = 1.29$) one gets $T_{\rm veil} \sim 3400\,$K. Taking the individual $r_{\rm J}$s and $r_{\rm K}$s for each star and the appropriate $T_{\rm eff}$ one finds $T_{\rm veil}$ ranging from $2100\,$K to $4800\,$K. For most stars $T_{\rm veil}$ is between 3000 and $4000\,$K (see Folha 1998 for $T_{\rm veil}$ for individual stars).

Temperatures similar to these are expected to occur in the innermost regions of accretion disks, i.e. $R/R_* < 3$, if inner disk holes are not present (Meyer et al. 1997). However as the dust sublimation temperature is $\sim 1,500\,$K (see Meyer et al. 1997) the continuum cannot be due to dust, so the presence of a continuum approximating a blackbody is unlikely.

Martin (1996) determined the thermal structure of magnetic accretion flows in TTS and concluded that the temperature of the gas in the flow is typically between 3000 and 6000 K, depending on the region of the flow. Calvet & Gullbring (1998) present models where this veiling continuum arises from shocks at the base of magnetospheric accretion columns.

7.2. An accretion shock origin for the Veiling

The veiling observed at optical wavelengths is usually explained by radiation which, in the Boundary Layer accretion model is thought to arise in the boundary layer itself (Basri & Bertout 1989), and in the Magnetospheric accretion model is thought to result from the accretion shock (Guenther & Hessman 1993, Calvet & Gullbring 1998).

Weak Line T Tauri stars (WTTS), being non or weakly accreting objects, should have zero or nearly zero veiling. From Table 1 we see that WTTS are indeed not significantly veiled.

To investigate the relationship between the veiling at V and our IR veilings, Fig. 8 plots the V veiling obtained by Gullbring et al. (1998) and by Hartigan et al. (1995) versus the J and K veiling obtained here. Some degree of correlation is present as the higher the veiling at V the higher the NIR veiling. Models where the veiling continuum arises from a shock at the base of a magnetospheric accretion column imply that the shock veiling in the NIR should be 0.1 that at V for values of $\mathcal{F}$ (the energy flux of the accretion flow in ergs cm^{-2} s^{-1}) of $\log \mathcal{F} = 11.5$ (Calvet & Gullbring 1998). However the dotted line in Fig. 8 indicates that this is not what is shown by our observations. Calvet & Gullbring (1998) also present a model with a smaller accretion energy flux ($\log \mathcal{F} = 10.5$) for which the NIR veiling relative to V is close to 0.6. Our observations are much better fitted by this value shown as a solid line in Fig. 8.

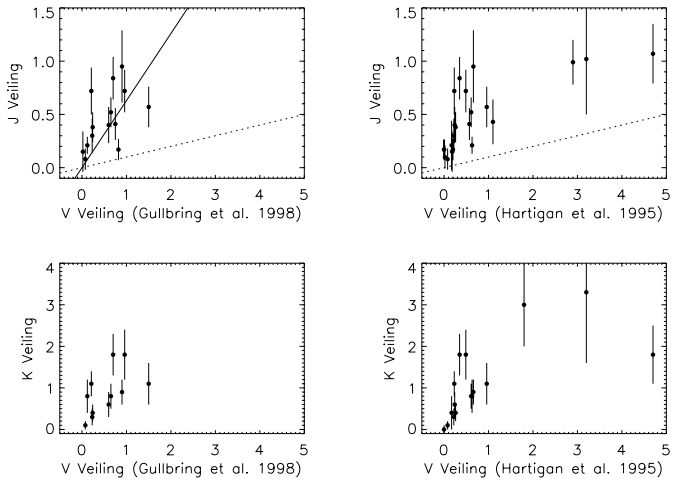

Fig. 8. Optical versus near NIR veiling. On the left hand side panels the optical veiling computed by Gullbring et al. (1998) is plotted against the J veiling (upper panel) and against the K veiling (lower panel) computed in this work. The right hand side panels are similar to the ones on the left for optical veiling computed by Hartigan et al. (1995). The dotted lines on the top panels represent $r_{\rm J} = 0.1\, r_{\rm V}$, and the solid line $r_{\rm J} = 0.63\, r_{\rm V}$. The best fitting straight line is $r_{\rm J} = 0.17 + 0.20 r_{\rm V}$. The NIR and V veiling measurements were made at different epochs, so variability will confuse any relation.

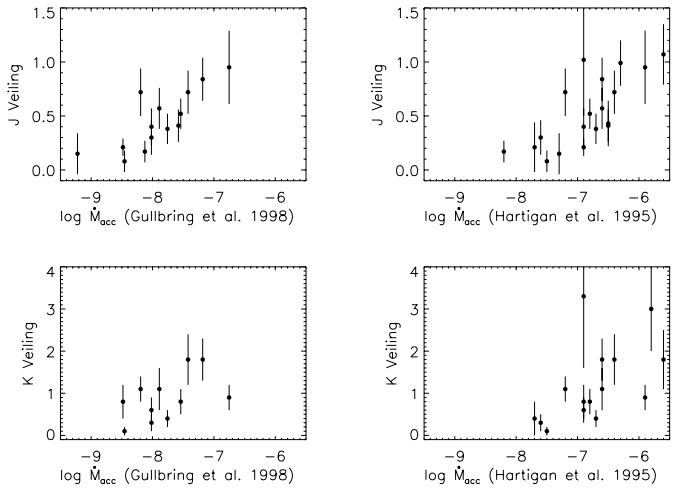

Fig. 9. Mass accretion rates, as determined by Gullbring et al. (1998) and by Hartigan et al. (1995) versus NIR veiling. The plots on the left hand side panels use the Gullbring et al. $\dot{\rm M}_{acc}$ while those on the right hand side use Hartigan et al.'s. The J veiling is on the top panels and the K veiling on the lower panels. The uncertainty on $\dot{\rm M}_{acc}$ is about a factor of 3 (Gullbring et al. 1998 and Hartigan et al. 1995).

However to match the absolute value of our IR veilings with the $\log \mathcal{F} = 10.5$ model that gives about the right ratio of veiling at J relative to at V would require a filling factor f for the accretion columns of around 0.9 according to Fig. 11 of Calvet & Gullbring (1998). Such a high filling factor is much greater even than the values required to fit the optical veiling of continuum stars. This model is able to explain the optical and IR observations simultaneously only if the filling factor in the IR is much larger than in the optical.

Thus these accretion shock models do not easily explain our measured J & K veilings which are much higher than expected if they are only due to same accretion shock responsible for the veiling at V. The emission responsible for the NIR veiling may therefore have a different origin to the optical veiling.

Fig. 9 plots the mass accretion rate, as determined by Gullbring et al. (1998) and by Hartigan et al. (1995), versus our J and K veiling. The J veiling correlates well with the mass accretion rate. A similar correlation might occur with the K veiling, however the large uncertainties make it difficult to make a clear judgement. The $\dot{\rm M}_{acc}$ vs. $r_{\rm J}$ correlation is further enhanced by noting that CW Tau, DG Tau, DR Tau and YY Ori, in which photospheric features are not detected in the J-band spectra presented here, therefore implying high veiling at J (these four objects have lower limits on $r_{\rm J}$ larger than one), all have $\dot{\rm M}_{acc} \geq 10^{-6}\, {\rm M}_{\odot}\, {\rm yr}^{-1}$, as determined by Hartigan et al. (1995).

Most of our stars showing clear veiling are in the narrow spectral type range K7-M1. One then expects the NIR veiling to correlate with the mass accretion rate either if the veiling arises in a shock, or if from a circumstellar disk, since in the latter case the higher the accretion rate the higher the disk temperature at a given radius implying that the disk becomes more capable of producing the NIR veiling (Meyer et al. 1997).

7.3. Circumstellar accretion disk as source of the veiling

To investigate the likelihood of emission from the accretion disk providing the IR veiling we note that Meyer et al. (1997) modelled accretion disks around an M0 star and predicted the contribution of the disk to the continuum veiling in the J, H, K and L bands. They then compare the results with those expected for the shock veiling at these wavelengths, by assuming that the veiling at J is one tenth the veiling at V, and that there is no veiling due to the disk at J. Their results (averaged over an appropriate range of accretion rates, stellar masses and inclinations) are shown as cumulative histograms in their Fig. 6 and those for J and K are reproduced here in our Fig. 10.

The heavy solid lines in Fig. 10 correspond to the veilings at J and K (distributions shown in Fig. 6). Comparing these measurements with the model predictions indicate that small ($< 2R_*$) inner hole sizes are typically needed to explain our observations by this mechanism.

The heavy dashed lines in Fig. 10 correspond to the distributions for the J and K veiling obtained by adding the solid and the dashed lines in Fig. 6 to take account of the objects with only lower limits on the veiling. This corresponds to the conservative assumption that the veiling in the stars for which only lower limits were obtained is the actual lower limit. As expected, the heavy dashed lines reinforce the fact that disks with small ($< 2R_*$) hole sizes would be needed in order to explain the observations. The stars for which only lower limits were obtained may well have $r_{\rm J}$ and $r_{\rm K}$ higher than the lower limit itself. In that case, the veiling distributions will be enhanced even fur-

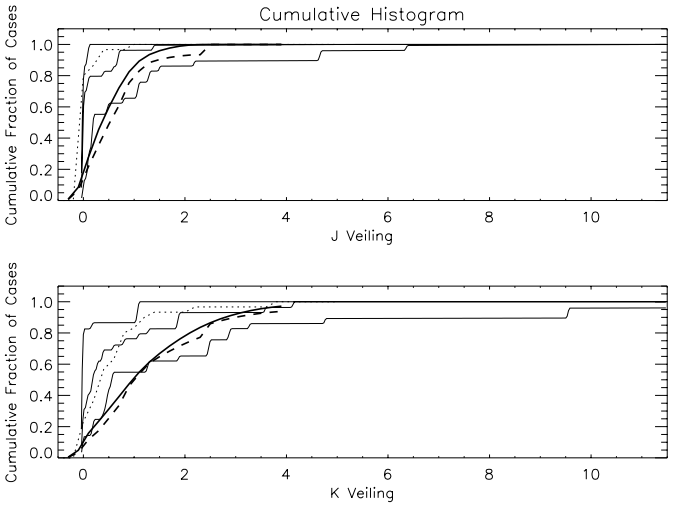

Fig. 10. *Top panel:* The lighter solid lines are a reproduction of the model results from Meyer et al. (1997) for the veiling at J produced by a circumstellar disk without a inner hole (lower thin line), with intermediate sized inner holes ($2R_* < R_{hole} < 6R_*$) (middle thin line), and with a large sized inner holes ($R_{hole} = 8R_*$) (upper thin line). The heavy solid lines correspond to $r_{\rm J}$ obtained from the distributions represented by solid lines in Fig. 6; the heavy dashed lines include the contribution from the stars for which only lower limits were obtained (from distributions in Fig. 6); the dotted line is the result obtained from broad band photometry with the assumption that the veiling in the NIR is due exclusively to the accretion shock, i.e. $r_{\rm J} = 0.1\, r_{\rm V}$. *Bottom panel:* same as top for K veiling.

ther for high values of the veiling, implying that the dashed line reaches unity at even larger values for the veiling.

Even disks without inner holes (which would be in conflict with expectations from the generally successful magnetospheric accretion model) can be incapable of explaining the high veiling observed at J and K. Meyer et al. (1997) show computed NIR spectra (for $i = 60°$) from circumstellar disks around TTS. With the disk extending right to the surface of the star the disk contribution at the J-band only exceeds that of the photosphere ($r_{\rm J}(disk) > 1$) for mass accretion rates $> 3 \times 10^{-7}$ $\rm M_\odot\ yr^{-1}$. At mass accretion rates $< 3 \times 10^{-7}$ $\rm M_\odot\ yr^{-1}$, thought typical of most TTS (Gullbring et al., 1998), the disk contribution at the J-band is less than that of the stellar photosphere. The disk emission in the NIR should be even smaller than this though, since the presence of inner disk holes, as expected for magnetospheric accretion scenarios, remove the hotter regions of the disk which are responsible for the emission at these wavelengths. The expected veiling at J due to a circumstellar disk with a inner hole of size $4R_*$ and for accretion rates typical of those in TTS is < 1. The expected veiling at K is, in these circumstances, smaller than 0.1 (Calvet, private communication). We thus conclude that emission from the accretion disks that are envisioned to surround TTS does not explain our results.

Calvet et al. (1997) calculate values for $r_{\rm J}$ similar to those reported here for veiling by thermal emission of an infalling dusty envelope around a star and disk system. However a significant envelope is characteristic of Class I sources but is apparently not present around most TTS, as witnessed by their optical visibility. Also, the $r_{\rm K}$ predicted by Calvet et al. are much higher than measured in this work, further suggesting that heated dust in an envelope is not the origin of our high veilings.

We thus conclude that neither emission from the shock, nor from the accretion around the star, can readily explain our measurements.

7.4. Veiling due to emission lines

The optical veiling has implicitly been assumed to result from an extra source of continuum emission. Despite that, as shown by Hartigan et al. (1989), for a few photospheric lines in the optical spectra of BP Tau there is also a small contribution from line emission, possibly of chromospheric origin. Could the NIR veiling we observe be due to line emission rather by a continuum source of radiation? Fig. 4 shows that the luminous (53 $L_\odot$, McMuldroch et al. 1993) star V1331 Cyg, which appears to be intermediate between a T Tauri and an Herbig Ae-Be star, has the photospheric lines not in absorption but in emission. Biscaya et al. (1997) show that its 2.3 μm $\Delta\nu = 2$ CO bands are in emission and that at the time of their observations their equivalent width doubled within 9 days. Although V1331 Cyg is somewhat different from the rest of our sample, this suggests that in the other CTTS the photospheric lines we use here to determine the veiling may also have an emission component which might contribute to the relatively high NIR veiling observed. Such line emission could arise in the atmosphere of the accretion disk, or in the accretion columns or shocks. It is however unlikely to arise in the fast wind as, at our spectral resolution, we would easily separate the stellar and wind velocities. To further investigate the possibility of line emission being the veiling source it is important that model calculations which include these lines be made to see if they can explain our observations.

8. Conclusion

The data presented here allows one to determine J and K continuum veiling for T Tauri stars (TTS) from photospheric features. The method used is independent of any assumption about the extinction/reddening towards the individual objects.

The observed Weak Line TTS (WTTS) show $r_{\rm J}$ measurements compatible with zero.

Relatively large values for near infrared (NIR) veiling are found here for several Classical TTS (CTTS). Average values of veiling for all the CTTS are $\langle r_{\rm J}\rangle = 0.57$ and $\langle r_{\rm K}\rangle = 1.29$. Considering only CTTS with veilings determined to better than 3σ these means are $\langle r_{\rm J}\rangle = 0.97$ and $\langle r_{\rm K}\rangle = 1.76$.

In addition to the actual values determined for $r_{\rm J}$ and r_K, a number of CTTS with photospheric lines detected in the optical show no signs of photospheric lines in the NIR regions observed. Considering only those CTTS with lower limits to the veiling the mean lower limits are $\langle r_{\rm J}\rangle > 1.34$ and $\langle r_{\rm K}\rangle > 2.4$.

Even if there is some systematic spectral type mismatch between out CTTS and our templates it is clear that a significant number of CTTS have relatively high values of $r_{\rm J}$ and $r_{\rm J}$.

The origin of such high veiling at these NIR wavelengths is not easily explained either by the accretion shock that is thought to give rise to optical veiling, or by accretion disks with inner holes. Both are expected to exist in the currently favoured magnetospheric accretion model. A model where accretion columns carrying an energy flux $\log \mathcal{F} = 10.5\,\mathrm{ergs\,cm^{-2}\,s^{-1}}$ (Calvet & Gullbring, 1998) and filling 90% of the stellar surface could just about explain our observations, but the high filling factor is inconsistent with the idea of isolated magnetospheric accretion columns, and so we do not adopt this as a likely explanation. The relationships between the amount of veiling observed in the optical and that observed at J and K, together with the correlation observed between the mass accretion rate and $r_{\rm J}$ and $r_{\rm K}$ indicate that wherever the extra emission arises it is closely linked with the accretion process.

Perhaps continuum or line emission resulting from within the accretion flow itself, or line emission from the shock at its base or from the atmosphere of the accretion disk might be the source of the radiation veiling the NIR photospheric lines of CTTS. Further modelling which includes opacity sources relevant to our observed region of spectrum (i.e. including Ti, Fe, Si, Mn) is required to study these possibilities.

It is also important to perform a further careful study of the veiling in the NIR for both WTTS and CTTS in order to extend and confirm these results and to eliminate possible sources of systematic errors. A careful choice of photospheric lines and the observation of a good grid of template stars should decrease the uncertainties in the veilings. The NIR veiling is, for the sample of stars studied here, higher than what has been suspected thus far and current models do not seem to be able to easily explain the origin of this NIR continuum veiling.

Acknowledgements. We would like to thank Nuria Calvet for sharing results and J.F.Gameiro for showing us a spectrum of V1331 Cyg, both prior to publication, and Lee Hartmann and Nuria Calvet for helpful discussions. D.F.M.Folha acknowledges financial support from the "Subprograma Ciência e Tecnologia do 2^o Quadro Comunitário de Apoio". The United Kingdom Infrared Telescope, is operated by Joint Astronomy Centre on behalf of the U.K. Particle Physics and Astronomy Research Council.

Appendix A: histograms – method for computation

Ideally a histogram would have a bin size with width Δ larger than the uncertainties in the parameters. This can make analysis more difficult due to the relatively large bin width that would have to be used. To overcome this problem we chose a bin of width Δ and compute the probability for a measurement of the parameter to fall inside it, by assuming that a measurement results from a normal probability distribution with mean equal to the measured value and with standard deviation equal to the uncertainty in the measurement, that is,

$$f(x) = \frac{1}{\sigma\sqrt{2\pi}} e^{-\frac{(x-\mu)^2}{\sigma^2}} \tag{A1}$$

where, μ is the measured value and σ its uncertainty.

The height of a given bin is now the sum of the probabilities of all the measurements, i.e.

$$h_j = \sum_{i=1}^{N} \int_{x_0}^{x_1} \frac{1}{\sigma_i\sqrt{2\pi}} e^{-\frac{(x-\mu_i)^2}{\sigma_i^2}}\, dx \tag{A2}$$

where, h_j is the height of bin *j* in the histogram, N is the number of measurements of the parameters, x_0 and x_1 are the end points of the bin, σ_i and μ_i, i=1...N, are the measurements of the parameter under study for the various stars and their associated uncertainties.

The histogram is simply the values h_j for all bins considered. In the limit where the uncertainties tend to zero ($\sigma_i \to 0$) one recovers the usual histogram.

References

Basri G., Batalha C., 1990, ApJ, 363, 654
Basri G., Bertout C., 1989, ApJ, 341, 340
Biscaya A.M., Rieke G.H., Narayan G., Luhman K.L. & Young E.T., 1997, ApJ, 491, 359
Calvet N., Hartmann L., Strom S. E., 1997, ApJ, 481, 912
Calvet N., Gullbring E., 1998, ApJ, 509, 802
Casali M., Eiroa C., 1996, A&A, 306, 427
Chelli A., 1999, A&A, 342, 763
Chelli A., Carrasco L., Mújica R., Recillas E. and Bouvier J., 1999, A&A, 345, L9
Folha D. F. M., 1998, Ph.D. thesis, Queen Mary & Westfield College, University of London, United Kingdom (Available on-line at URL: www.astro.up.pt/users/dfmf/Thesis/thesis.html
Ghez A. M., Neugebauer G., Gorham P. W., Haniff C. A., Kulkarni S. R., Matthews K., 1991, AJ, 102, 2066
Ghez A. M., Neugebauer G., Matthews K., 1993, AJ, 106, 2005
Ghez A. M., White R. J., Simon M., 1997, ApJ, 490, 353
Greene T. P., Lada C. J., 1996, AJ, 112, 2184
Greene T. P., Meyer M. R., 1995, ApJ, 450, 233
Guenther E., Hessman F., 1993, A&A, 268, 192
Guenther E., Lehmann H., Emerson J. P., Staude J., 1998, A&A, 341, 768
Gullbring E., Hartmann L., Briceño, C., Calvet N., 1998, ApJ, 492, 323
Hartigan P., Hartmann L., Kenyon S., Hewett R., Staufer J., 1989, ApJS, 70, 899
Hartigan P., Kenyon S. J., Hartmann L., Strom S. E., Edwards S., Welty A. D., Staufer J., 1991, ApJ, 382, 617
Hartigan P., Edwards S., Ghandour L., 1995, ApJ, 452, 736
Herbig G. H., Bell K. R., 1988, Third Catalogue of Emission-Line Stars of the Orion Population, Lick Observatory Bulletin Series No. 111, Lick Observatory, Board of Studies in Astronomy & Astrophysics, Univ. of California, Santa Cruz
Horne K., 1986, PASP, 98, 609
Leinert C., Zinnecker H., Weitzel N., Christou J., Ridgway S. T., Jameson R., Haas M., Lenzen R., 1993, A&A, 278, 129
Livingston W., Wallace L., 1991, An Atlas of the Solar Spectrum in the Infrared from 1850 to 9000 $\mathrm{cm^{-1}}$ (1.1 to 5.4 μm), National Solar Observatory Technical Report #91-001, Tucson, National Optical Astronomy Observatories
McMuldroch S., Sargent A.I., Blake G.A., 1993, AJ, 106, 2477
Martin S. C., 1996, ApJ, 470, 537
Mathieu R. D.: 1994, ARA&A, 32, 465

Meyer M. R., Ph.D. thesis, University of Massachusets, Amherst, 1996
Meyer M. R., Calvet N., Hillenbrand L. A., 1997, AJ, 114, 288
Puxley P. J., Beard S. M., Ramsey S. K., 1992, in P. Grosbøl & R. de Ruijsscher (eds.), 4^{th} ESO/ST-ECF Data Analysis Workshop, ESO Conference and Workshop Proceedings No. 41, p. 117
Richichi A., Leinert C., Jameson R., Zinnecker H., 1994, A&A, 287, 145
Ruedi I., Solanki S. K., Livingston W., Harvey J., 1995, A&AS, 113, 91
Simon M., Ghez A. M., Leinert C., Cassar L., Chen W. P., Howell R. R., Jameson R. F., Matthews K., Neugebauer G., Richichi, A., 1995, ApJ, 443, 625
Strom K. M., Strom S. E., Edwards S., Cabrit S., Skrutskie M., 1989, AJ, 97, 1451
Tonry J., Davis M., 1979, AJ, 84, 1511
Valenti J. A., Basri G., Johns C. M., 1993, AJ, 106, 2024
Wallace L., Hinkle K., 1996, ApJS, 107, 312